Alves Testoni, Samara; de Almeida, Jaime Antonio; da Silva, Luana; Ramatis Pugliese
Andrade, Gabriel
Clay Mineralogy of Brazilian Oxisols with Shrinkage Properties

Division - Soil Processes and Properties | Commission - Soil Mineralogy

Clay Mineralogy of Brazilian Oxisols with Shrinkage Properties

Samara Alves Testoni[1], Jaime Antonio de Almeida[2]*, Luana da Silva[1] and Gabriel Ramatis Pugliese Andrade[3]

[1] Universidade do Estado de Santa Catarina, Departamento de Solos e Recursos Naturais, Programa de Pós-Graduação em Ciência do Solo, Lages, Santa Catarina, Brasil.

[2] Universidade do Estado de Santa Catarina, Departamento de Solos e Recursos Naturais, Lages, Santa Catarina, Brasil.

[3] Universidade de São Paulo, Escola Superior de Agricultura Luiz de Queiroz, Departamento de Ciência do Solo, Programa de Pós-Graduação em Solos e Nutrição de Plantas, Piracicaba, São Paulo, Brasil.

ABSTRACT: Shrinkage capacity (*caráter retrátil* in Portuguese) is a new diagnostic characteristic recently introduced in the Brazilian System of Soil Classification (SiBCS) to indicate shrink and swell properties observed in subtropical soils from highland plateaus in southern Brazil, specifically in Oxisols with brown colors. In soils located in road cuts exposed to drying for some weeks, strong shrinkage of soil volume is observed in these soils, resulting in the formation of pronounced vertical cracks and large and very large prismatic structures, which crumble in blocks when handled. We hypothesize that such properties are related to their clay mineralogy, although there are no conclusive studies about this, the motive for the present study. Samples of the A and B horizons from six Oxisols with expansive capacity from the states of Santa Catarina and Rio Grande do Sul were analyzed. One Rhodic Hapludox, from the state of Paraná, without expansive capacity, was used for comparison. All the soils are very clayey, originated from basalt, and have similar iron oxide content. For identification of clay mineralogy, X-ray diffraction techniques were employed, together with the use of NEWMOD® software to investigate and describe the interstratified minerals. The results showed that most expansive soils have a similar mineralogical composition, with kaolinite, interstratified kaolinite-smectite (K-S), and hydroxy-Al interlayered smectites (HIS), unlike the non-expansive Rhodic Hapludox, which exhibited kaolinite with significant amounts of gibbsite and low amount of interstratified K-S. According to the mineralogical assemblage identified in the expansive soils, we can affirm that the mechanism of smectite expansion and contraction is related to the shrinkage capacity of the soil, considering that the level of hydroxy-Al intercalation is low. In addition, these mechanisms also are related to the presence of quasicrystals and domains that control the water dynamic in the smectites, contributing to shrinkage capacity.

Keywords: kaolinite-smectite, interstratified clay mineral, X-ray diffraction, quasicrystals.

INTRODUCTION

Shrinkage capacity (*caráter retrátil* in Portuguese), recently introduced in the Brazilian System of Soil Classification (SiBCS), is typical of some soils found in humid subtropical climate conditions of highland plateaus in southern Brazil, such as Oxisols with brown colors. In these soil classes, a marked shrinkage in the soil volume occurs after soil is exposed to drying conditions. Pronounced vertical cracks are formed, and large and very large prismatic structures develop, which crumble in blocks when handled. In road cuts exposed to sun for a few weeks, the blocks tend to naturally individualize in smaller structural units, accumulating at the surface of the profile, forming a triangular shape similar to a "skirt" (Santos et al., 2013).

Although kaolinite was identified as the dominant clay mineral in these soils, the shrinkage capacity, according to Santos et al. (2013), is possibly derived from 2:1 hydroxy-Al interlayered minerals, interstratified kaolinite-smectite (K-S), and/or to the small dimension of the clay mineral crystals. The cation exchange capacity (CEC) of these soils is low, but when the values were converted to clay content, it is situated between 8 to 15 $cmol_c$ kg^{-1} in the B horizons. Such values indicate low activity clays, but they are higher than many other purely kaolinitic or kaolinitic-oxidic Oxisols from other Brazilian regions. In addition, the value exceeds the kaolinite CEC, which generally has lower values (Giarola et al., 2009; Ryan et al., 2016), indicating a probable contribution of clay minerals with higher negative charge. This medium to high CEC may be a contribution from the 2:1 HIV (hydroxyl-interlayered vermiculite) or HIS (hydroxyl-interlayered smectite) clay minerals and/or a contribution from interstratified kaolinite-smectite in association with kaolinite, as suggested in the literature (Melo et al., 2009; Teske et al., 2013; Yongue-Fouateu et al., 2016). Dudek and Środoń (2006) found CEC values higher than 100 $cmol_c$ kg^{-1} for pure smectite, and values between 25 and 100 $cmol_c$ kg^{-1} for kaolinite-smectite with less than 10 % of kaolinite layers in the interstratified minerals.

Considering, therefore, that the soils studied have considerable proportions of 2:1 clay minerals and interstratified kaolinite-smectite, it could be that this contributes to the increase in soil CEC, even when in low proportions. If the hydroxy-Al intercalation in the 2:1 clay mineral is significant, however, the negative charges can be blocked, substantially reducing the natural CEC of the mineral (Kämpf et al., 2012), but maintaining the contraction and expansion properties. Such properties may also be related to variations in soil volume resulting from loss of water in microscopic aggregates with diameters from 1 to 2 µm, called quasi crystals or domains (several quasi crystals together), as proposed by Quirk and Aylmore (1971) and Tessier (1984).

The conceptual fragility of shrinkage capacity and current adoption of this characteristic as an essential criterion in definition of soil classes motivated the present study, with the aim of more accurately examining the causes and effects and relating them to soil mineralogy.

MATERIALS AND METHODS

Soil selection

Samples were taken from two horizons (A and B) of four Humic Hapludox (two *Latossolo Bruno Distrófico* and two *Nitossolo Bruno Distrófico*), two Typic Hapludox (one *Latossolo Vermelho Distroférrico* and one *Nitossolo Bruno Distroférrico*) with shrinkage capacity from the states of Santa Catarina and Rio Grande do Sul and one Rhodic Hapludox (*Latossolo Vermelho Distroférrico*) from Paraná without this capacity. All these soils developed from basalt rock, and their classification and location are described in table 1.

Table 1. Classification and location of the soils studied, correlated with soil taxonomy classification

Soil profile	Symbol	Horizon	SiBCS[1]	Soil taxonomy – Coordinate	Location
P1	LBdf$_{VAC}$	A B	*Latossolo Bruno Distroférrico*	Humic Hapludox 28° 30' 47.40" S; 50° 53' 36.90" W	Vacaria, RS
P2	LVdf$_{CN}$	A B	*Latossolo Vermelho Distroférrico*	Typic Hapludox 27° 22' 21.76" S; 51° 15' 44.89" W	Campos Novos, SC
P3	NBdf$_{CUR}$	A B	*Nitossolo Bruno Distroférrico*	Typic Hapludox 27° 22' 12" S; 50° 34' 46" W	Curitibanos, SC
P4	NBd$_{PS}$	A B	*Nitossolo Bruno Distrófico*	Humic Hapludox 26° 51' 22.9" S; 52° 02' 32.71" W	Ponte Serrada, SC
P5	LBd$_{VAR}$	A B	*Latossolo Bruno Distrófico*	Humic Hapludox 26° 51' 13.3" S; 52° 05' 56" W	Vargeão, SC
P6	NBd$_{PAI}$	A B	*Nitossolo Bruno Distrófico*	Humic Hapludox 27° 53' 41.8" S; 50° 07' 45" W	Painel, SC
P7	LVdf$_{CAS}$	A B	*Latossolo Vermelho Distroférrico*	Rhodic Hapludox 24° 59' 45.16" S; 53° 17' 44.61" W	Cascavel, PR

[1] SiBCS: Brazilian System of Soil Classification.

Physical analyses

For determination of the sand, silt, and clay fractions, the soil samples were treated with 1 mol L^{-1} NaOH for dispersion (Jackson, 1965). After removal of the sand fraction using a sieve with a 0.053 mm mesh, the clay fraction was separated from silt by sedimentation processes, based on Stokes law. Part of this clay fraction, designated as total clay (TC), was oven dried and stored. Another portion of the clay was fractionated into coarse clay (CC) and fine clay (FC) using centrifugation, according to Jackson (1965). These fractions were oven dried, the proportions in each sample were quantified, and the fractions were stored.

Pretreatments and mineralogical analysis

After fractionation, the iron oxides of the samples of the TC, CC, and FC fractions were removed by three successive extractions with sodium dithionite-citrate-bicarbonate (DCB), according to Mehra and Jackson (1960). A portion of each fraction was saturated with potassium (1 mol L^{-1} KCl), and another portion with magnesium (1 mol L^{-1} MgCl$_2$).

Mineralogy was characterized by X-ray diffraction (XRD). All the samples were analyzed on slides of oriented clay, using an X-ray diffractometer, Philips PW 1830, computer-controlled and equipped with a graphite monochromator and vertical goniometer. The radiation source used was Cu Kα, and the equipment was operated at 30 kV and 30 mA. The angular range of the radiation was from 3 to 44° 2θ, with a range of 0.01° 2θ for each 1 s. For some treatments, different radiation ranges were used.

The samples saturated with K were read at room temperature and after heating to 100, 350, and 550 °C for 4 h. The samples saturated with Mg were read at room temperature and after solvation with ethylene glycol. All these procedures were performed according to Whittig and Allardice (1986). Tests were also conducted for the presence of halloysite 0.7 nm with formamide spray solution, according to Churchmann et al. (1994). As there was no modification in the position and the intensity of reflections around 0.72 nm, the presence of this mineral was discarded.

Minerals were identified according to the criteria of Brown and Brindley (1980) and according to the supplementary literature indicated below.

Estimate of clay minerals

The quantity of clay minerals and gibbsite were estimated with the HighScore Plus software (Panalytical) by estimating the area of the major reflections of these minerals. This estimation was made in the total, fine, and coarse clay samples saturated with Mg, using the fitprofile tool. Special attention was given to the peaks at approximately 1.4 nm, corresponding to the expansive phyllosilicates with the 2:1 layer, and at approximately 0.72 nm, corresponding to the *001* basal peaks of kaolinite, but possibly also to interstratified kaolinite-smectite. From the shape and average position of the peak, mathematically calculated by the software, we obtaine the crystallographic parameters MCD (Mean Crystal Dimension), ANL (Average Number of Layers), WHH (Width at Half Height), and AI (Asymmetry Index) for kaolinite. These parameters cannot adequately represent the real crystallographic parameters of kaolinite, since only one mineral (kaolinite), with peak position at approximately 0.72 nm, was considered. However, we hypothesized that peaks of two minerals may be present.

For the kaolinite MCD_{001} calculation, the Scherrer's equation was used (Srodoń et al., 2006). The ANL was calculated by dividing the corresponding value of the MCD_{001} by the mineral spacing in the same *hkl* plane (in nanometers). Finally, the relative values of the AI were obtained by drawing a perpendicular line from the sharpest point of the *001* peak (summit) of the diffraction pattern to its baseline, measuring the width of the peak to the right and to the left at exactly half the height of the peak and, based on these values, the AI were calculated according to Melo and Wypych (2009).

Kaolinite and interstratified discrimination

The percentage of each mineral phase identified in the clay fraction was estimated from peak areas using Newmod[®] (Reynolds Jr, 1985) and HighScore Plus software. Serpentine was used to simulate kaolinite, serpentine-smectite was selected to simulate kaolinite-smectite, and chlorite was used to simulate hydroxy-Al interlayered smectite. Serpentine was chosen due to the presence of Fe in the samples that were not deferrified. The presence of Fe can reduce the intensity of kaolinite diffraction because Fe absorbs more radiation. The serpentine has Fe in their composition, attenuating the effect of reduction in intensity. In the simulation, previously known minerals are selected as phases in the software. For each phase, specific parameters were able to be adjusted, such as crystallinity level or atoms of Fe and K, depending on the mineral. For simulation of the type of interstratified minerals, the proportion of each mineral phase in the interstratified minerals that best fit the real diffractograms was selected by trial and error, for example 90 % of the kaolinite phase and 10 % of the smectite phase. For simulation of the 2:1 layer minerals, only the diffractograms of the samples saturated with Mg were considered.

The patterns obtained by NEWMOD[®], estimate the composition of the simple clay minerals and the mixed layers (interstratified) and identify them.

RESULTS AND DISCUSSION

Total clay fraction mineralogy

In almost all soil samples with shrinkage capacity studied from the A and B horizon, the mineralogical composition of the total clay fraction was similar. The most intense, wide, and asymmetric peak occurred at *d* values around 0.72 and 0.36 nm, positions typically attributed to *001* and *002* kaolinite basal planes (Brown et al., 1978; Barnhisel and Bertsch, 1989); this was seconded by less intense peaks, with *d* values of around 1.42 nm, usually indicating 2:1 expansive phyllosilicates or chlorite (Azevedo and Vidal-Torrado, 2009). Peaks around 0.48 and 0.43 nm, attributed to gibbsite, and at 0.27 nm, attributable to goethite and hematite, with low intensity in most samples, were also detected (Figure 1). In the Rhodic Hapludox profile from Cascavel (PR), although peaks in the kaolinite position predominated,

more intense peaks were observed in the positions around 1.42 and 0.48 nm, indicating expressive amounts of 2:1 phyllosilicate and gibbsite minerals, respectively (Figure 1). This behavior denotes mineralogical differences of this soil in relation to the others.

The large width of kaolinite peaks may be indicative of a small crystal size (Klug and Alexander, 1954; Wilding and Tessier, 1988; Melo et al., 2001) and also high structural disorder of these minerals. This disorder may be related to the high iron content in kaolinites (Lima Neto et al., 2010), given that all the soils are developed from basalt. In contrast, in all horizons with expansive capacity, the peaks at the 0.72 nm position are broad and asymmetric toward lower 2θ angles, and in the 0.36 nm position, the asymmetry is toward higher 2θ angles. According to many authors (Azevedo and Vidal-Torrado, 2009; Fiore et al., 2010; Kämpf et al., 2012), this behavior usually indicates 2:1 layers interstratified in kaolinites crystals, probably kaolinite-smectite (K-S) (Melo et al., 2009).

Other tests and procedures have been utilized to investigate interstratified clay minerals in soils utilizing XRD techniques, such as the use of NEWMOD®, which obtain an estimate of interstratified minerals, indicating the proportion of some mineral that
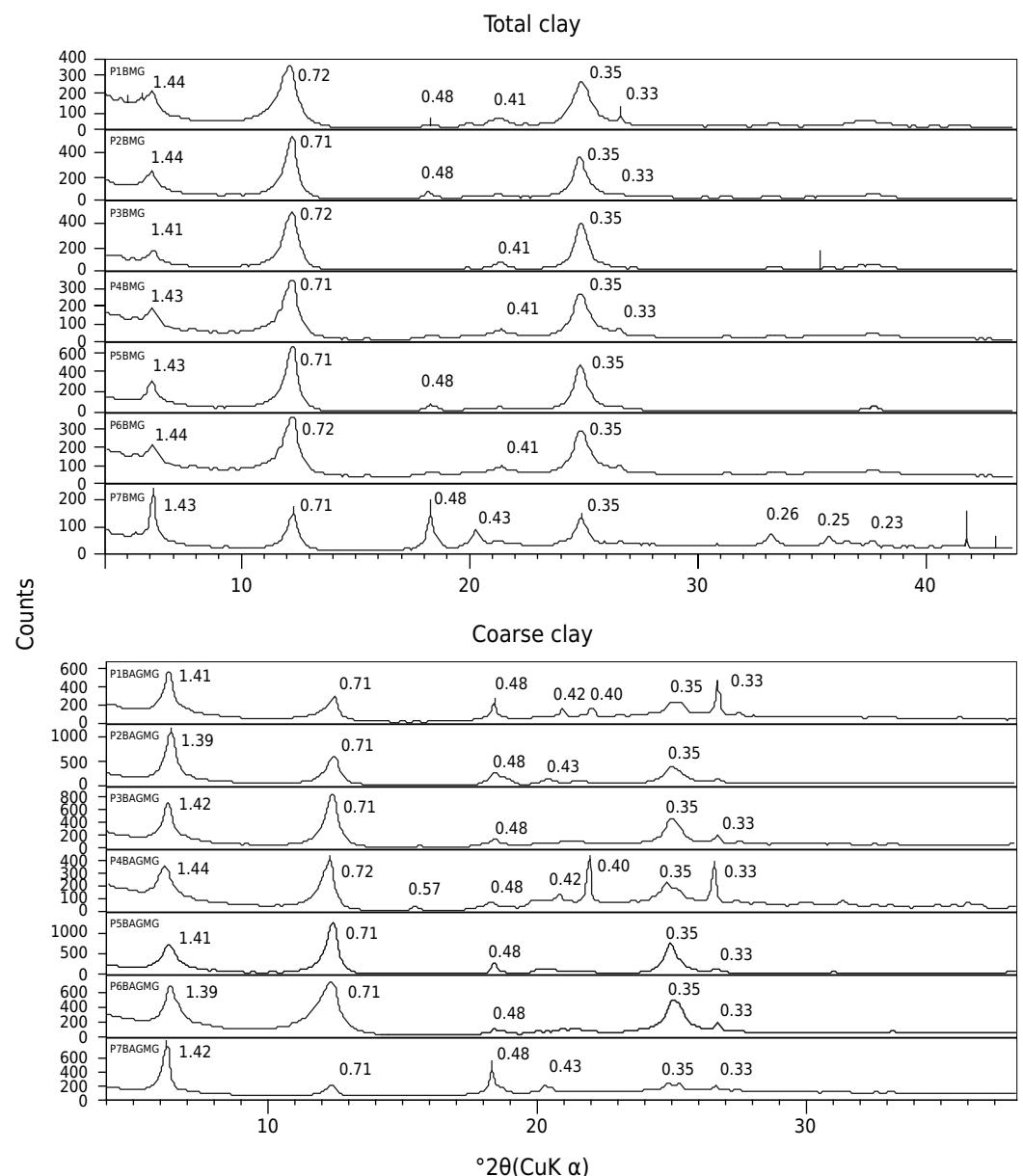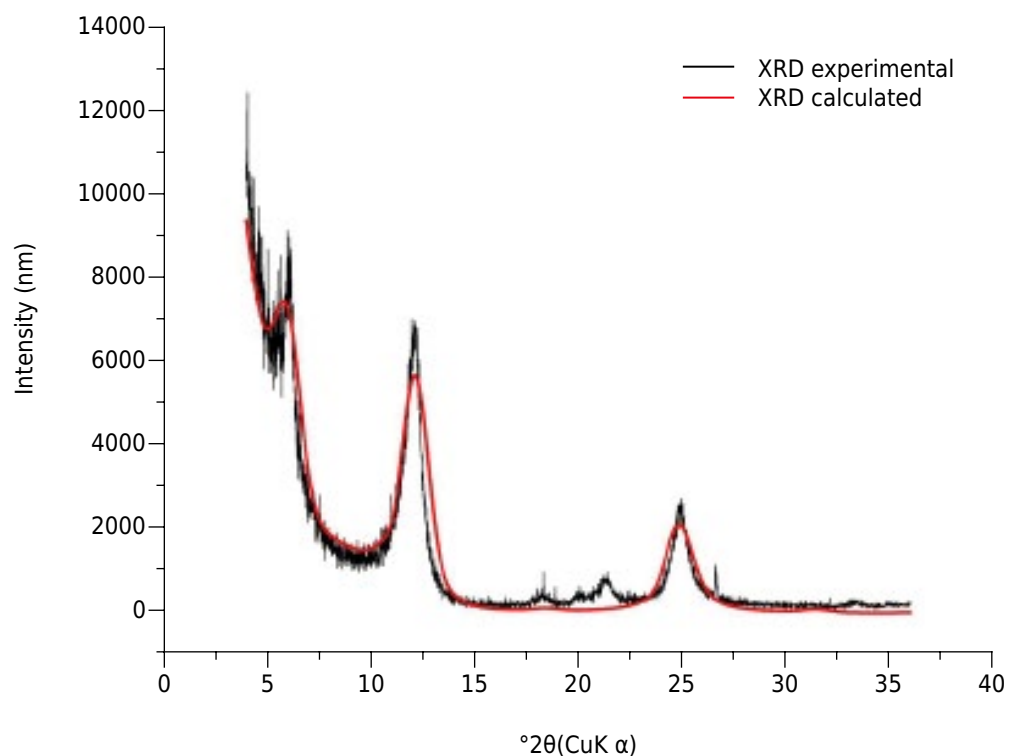

Figure 1. X-ray diffractograms of the total clay and coarse clay fraction samples from the B horizon, saturated with magnesium and read at ambient temperature in the seven soil profiles studied. Spacing values in nanometers (nm).

compounds the mixed layer mineral, according to the results of X-ray diffraction. The best simulations of mineral phases were performed when we consider the K-S phase with 5 and 10 % of smectite layers and 90-95 % of kaolinite layers, which is coherent with results obtained by other authors in more developed soils derived from basalt (Benedetti et al., 2011). An example of modeling performed by the software is shown in figure 2, containing the experimental diffractograms (obtained by XRD) and the calculated diffractograms (obtained by Newmod®).

However, the classic tests used for regular interstratified K-S identification, such as the positions of peak displacement after ethylene-glycol treatment or after thermal treatment (Środoń et al., 2006), did not promote any modification in the position of peaks in the positions mentioned. This was probably because they are not regular interstratified minerals and/or the 2:1 interlayer spaces have Al polymers entrapped in them, and possibly due to the reduced amount of these minerals in the samples analyzed. Thus, it was not possible to confirm the presence and the proportion of the interstratified minerals in the expansive soil samples with only the traditional XRD tools.

For all solvated ethylene glycol samples, there was no change in the 1.4 nm peak position in relation to peak positions of Mg saturated samples, indicating that the minerals may be chlorites or 2:1 phyllosilicates with hydroxyl-Al interlayer polymers (2:1 HI) (Azevedo and Vidal-Torrado, 2009). For most soils and horizons analyzed, heating potassium samples to 350 and 550 °C caused an incomplete collapse of the layers (data not shown), confirming 2:1 layer phyllosilicates that can be HIS or HIV. Similar results were obtained by Herbillon et al. (1981) and Yerima et al. (1985) in acid basalt soils, where HIS was the main 2:1 layer mineral identified.

After heating to 550 °C, the most acute peak position occurred at values near 1.10 nm, indicating that 2:1 HI phyllosilicates have strong hydroxy-Al polymer intercalation in the interlayer. At this temperature, the reflections in 0.72 and 0.36 nm disappeared, confirming kaolinite destruction (and/or destruction of the kaolinite portion of interstratified K-S).

Figure 2. Comparative between experimental diffractogram (obtained by X-ray diffraction) and calculated diffractogram (obtained through NEWMOD®) referred to the Profile 1, B horizon, total clay fraction of *Latossolo Bruno* from Vacaria, RS (LBVAC).

It was not possible, however, to determine the nature of the 2:1 layer phyllosilicates, if they are smectite or vermiculite.

Mineralogy of fine and coarse clay fractions

According to the estimate made from the HighScore Plus software, the mineralogical components in both clay fractions were the same as found in the total clay fraction, with kaolinite, 2:1 phyllosilicate with hydroxy-Al interlayers, and possibly interstratified kaolinite-smectite; in minor amounts, gibbsite, quartz, and iron oxides were found. However, there is a substantial change in the proportion of the components. For most samples in the coarse clay fraction, the amount of 2:1 phyllosilicates was superior, sometimes exceeding the amount of minerals with the *001* peak position of kaolinite (Figure 3 and Table 2).

Like the total clay fraction, the collapse of 2:1 layers by heat treatments was incomplete, with the central peak position located between 1.05 and 1.15 nm. The glycolate samples showed no perceptible expansion either, which corroborates the hypothesis of considerable intercalation of hydroxy-Al polymers that prevent and/or reduce this expansion. In the A and B horizons of fine and coarse clay samples of the P4 and P5 profiles, however, a slight expansion was observed, confirmed by the background elevation between 1.4 to 1.6 nm. In the same horizons of the P6 profile, in the coarse and fine clay, the glycolation retained most of the reflex around 1.4 nm, but a small peak was formed near 1.66 nm (data not shown), which suggests that the basic structure of the 2:1 phyllosilicates is a smectite compound. These results are contradictory in a way, since the smectite crystallites were generally very small, and thereby most commonly found in fine clay. Kämpf et al. (2012), however, questioned the occurrence of vermiculite in soils developed from basalt, since these clay mineral are mostly developed from mica transformation. Micas in the basalts of southern Brazil have been reported to be little expressive, so the presence of HIV in soils derived from these rocks would be unlikely.

Estimation of the amount of mineral phases in the clay fractions through the relative calculations of peaks areas were performed with the HighScore Plus software and refer to an approximation of the percentages of each phase in the total, fine, and coarse clay fractions (Table 2).
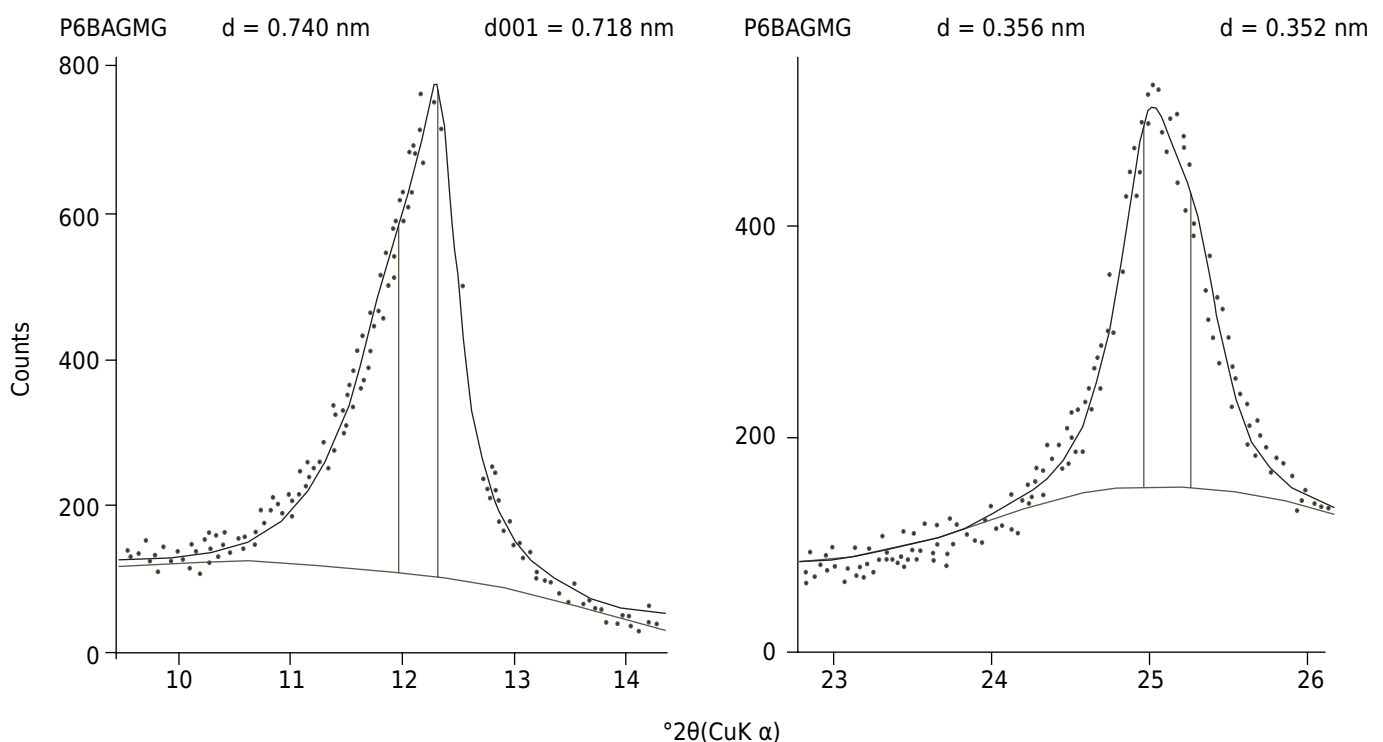
Figure 3. Automatic simulation of the shape of peaks in *hkl 001* and *002* plans of "kaolinite" in the coarse clay sample from the B horizon of profile 6 [*Nitossolo Bruno* (Oxisol), Painel, SC] with the use of HighScore Plus software.

Table 2. Values related to the percentages of each mineral in the clay fraction, calculated by HighScore Plus software and obtained from estimates of the peak areas in the respective peak positions (1.42 nm, 0.72 nm, and 0.48 nm) for total, fine, and coarse clay fractions

Profile[1]	Horizon	Total clay			Fine clay			Coarse clay		
		1.42 nm	0.72 nm	0.48 nm	1.42 nm	0.72 nm	0.48 nm	1.42 nm	0.72 nm	0.48 nm
						%				
P1 - LB$_{VAC}$	A	31.0	69.0	-	14.0	86.0	-	54.0	46.0	-
	B	22.0	78.0	-	10.0	90.0	-	59.0	41.0	-
P2 - LV$_{CN}$	A	18.0	82.0	-	11.0	89.0	-	56.0	44.0	-
	B	21.0	79.0	-	15.0	85.0	-	58.0	42.0	-
P3 - NB$_{CUR}$	A	16.0	84.0	-	5.0	95.0	-	38.0	62.0	-
	B	13.0	87.0	-	5.0	95.0	-	35.0	65.0	-
P4 - NB$_{PS}$	A	36.0	64.0	-	13.0	87.0	-	47.0	53.0	-
	B	15.0	85.0	-	-	-	-	37.0	63.0	-
P5 - LB$_{VAR}$	A	25.0	75.0	-	15.0	85.0	-	44.0	56.0	-
	B	20.0	80.0	-	12.0	88.0	-	34.0	66.0	-
P6 - NB$_{PAI}$	A	20.0	80.0	-	10.0	90.0	-	35.0	65.0	-
	B	20.0	80.0	-	15.0	85.0	-	29.0	71.0	-
P7 - LV$_{CAS}$	A	24.0	49.0	27.0	15.0	65.0	20.0	44.0	22.0	35.0
	B	31.0	43.0	27.0	20.0	59.0	21.0	58.0	16.0	26.0

[1] P1 - LB$_{VAC}$: *Latossolo Bruno* in Vacaria/RS; P2 - LV$_{CN}$: *Latossolo Vermelho* in Campos Novos/SC; P3 - NB$_{CUR}$: *Nitossolo Bruno* in Cutitibanos/SC; P4 - NB$_{PS}$: *Nitossolo Bruno* in Ponte Serrada/SC; P5 - LB$_{VAR}$: *Latossolo Bruno* in Vargeão/SC; P6 - NB$_{PAI}$: *Nitossolo Bruno* in Painel/SC; P7 - LV$_{CAS}$: *Latossolo Vermelho* in Cascavel/PR. -: not measured.

In the total clay fraction, high quantities of 2:1 clay minerals were observed, interpreted as HIS, ranging from 13 to 36 %, with an average value of 22 %. All the soils studied are very clayey, and this may contribute to the soil properties of contraction and expansion, even considering that this contraction is limited by interlayered Al polymers. In addition to this effect, the inflow and outflow of water in the pores created between the quasicrystals and in the set of quasicrystals (domains) may also contribute to the swell and shrink properties because the process of water leaving the interlayer space requires a great deal of energy (Quirk and Aylmore, 1971; Tessier, 1984), and this would hardly occur under natural drying conditions in the soil. Considering the clay fractions individually, the increase in 2:1 HI is clearly evident. Due to low expression of gibbsite peaks in shrinkage soil, it was not possible to measure their area, but their amount was relatively high in all the clay fractions of the non-expansive soil (Table 2).

Crystallographic "kaolinite" parameters

Traditionally, the presence of broad and asymmetric peaks in the 0.72 and 0.36 nm positions of derivatives basalt soils of southern Brazil has been interpreted as the result of disordered kaolinite, small size crystallites of this mineral (Klug and Alexander, 1954; Wilding and Tessier, 1988; Almeida et al., 2000; Melo et al., 2001), or even dehydrated halloysites (Palmieri, 1986), although some authors also interpret that the asymmetries may be due to the contribution of pure interstratified kaolinite-smectites, or to mixtures of pure smectites with pure kaolinites (Melo et al., 2009; Teske et al., 2013; Yongue-Fouateu et al., 2016). Starting from the presupposition that asymmetric reflections with values around 0.72 nm were due only to kaolinite, and based on HighScore Plus software, the main crystallographic parameters of this supposed mineral were calculated from the peak positions 0.72 e 0.36 nm for the clay fractions. The average values of the *hkl 001* and *002* spacing plans (d$_{001}$ and d$_{002}$) and the width of the reflection at half height in the *001* plan (WHH$_{001}$) were obtained automatically with the fitprofile resource of the HighScore Plus software, which considers the average position of the peaks after a mathematical treatment to simulate their shape (Table 3).

Table 3. Amounts referring to crystallographic parameters (WHH$_{001}$ - Width at Half Height in *001* plan; MCD$_{001}$ - Mean Crystal Dimension in the *001* plan, ANL - Average Number of Layers, and AI - Asymmetry Index) of "kaolinites" in the samples of the total clay (TC), fine clay (FC) and coarse clay (CC) samples in the A and B horizons of the profiles studied

Profile[1]	Hor[2]	d$_{001}$			d$_{002}$	WHH$_{001}$			MCD$_{001}$			ANL			AI		
		TC	FC	CC	TC	TC	FC	CC	TC	FC	CC	TC	FC	CC	TC	FC	CC
		⸻ nm ⸻				⸻ °2θ ⸻			⸻ nm ⸻								
P1 - LB$_{VAC}$	A	0.740	0.730	0.720	0.360	0.88	0.90	0.69	9.8	9.8	13.6	13.2	13.4	18.8	0.36	0.20	0.38
	B	0.730	0.720	0.720	0.360	0.88	0.94	0.61	10.0	9.4	15.7	13.6	13.0	21.9	0.22	0.17	0.38
P2 - LV$_{CN}$	A	0.730	0.720	0.720	0.360	0.86	0.75	0.60	10.5	12.2	16.0	14.4	16.9	22.2	0.17	0.14	0.30
	B	0.730	0.730	0.720	0.360	0.66	0.76	0.55	14.3	12.1	18.0	19.8	16.6	25.1	0.22	0.10	0.26
P3 - NB$_{CUR}$	A	0.730	0.720	0.720	0.360	0.71	0.73	0.56	13.0	12.6	17.5	17.8	17.4	24.3	0.14	0.10	0.20
	B	0.726	0.722	0.720	0.357	0.74	0.73	0.57	12.3	12.7	17.2	17.0	17.6	23.9	0.20	0.16	0.25
P4 - NB$_{PS}$	A	0.726	0.723	0.720	0.358	0.68	0.83	0.62	13.6	10.9	15.4	18.7	15.1	21.4	0.38	0.24	0.42
	B	0.726	-	0.728	0.358	0.79	-	0.58	11.5	-	16.7	15.8	-	23.0	0.34	-	0.28
P5 - LB$_{VAR}$	A	0.725	0.728	0.720	0.358	0.66	0.92	0.51	14.2	9.6	19.7	19.6	13.2	27.4	0.21	0.23	0.26
	B	0.724	0.724	0.718	0.358	0.65	0.72	0.50	14.5	12.9	20.1	20.0	17.8	28.1	0.20	0.10	0.23
P6 - NB$_{PAI}$	A	0.732	0.732	0.718	0.357	0.97	0.88	0.77	9.0	10.0	11.8	12.2	13.7	16.4	0.18	0.20	0.16
	B	0.734	0.731	0.727	0.357	0.95	0.90	0.93	9.1	9.8	9.5	12.4	13.5	13.0	0.18	0.12	0.20
P7 - LV$_{CAS}$	A	0.721	0.718	0.727	0.358	0.74	0.54	0.44	12.5	18.3	23.5	17.4	25.3	32.4	0.08	0.12	0.24
	B	0.722	0.727	0.720	0.358	0.60	0.56	-	16.3	17.5	-	22.4	24.1	-	0.13	0.16	-

[1] P1 - LB$_{VAC}$: *Latossolo Bruno* in Vacaria/RS; P2 - LV$_{CN}$: *Latossolo Vermelho* in Campos Novos/SC; P3 - NB$_{CUR}$: *Nitossolo Bruno* in Cutitibanos/SC; P4 - NB$_{PS}$: *Nitossolo Bruno* in Ponte Serrada/SC; P5 - LB$_{VAR}$: *Latossolo Bruno* in Vargeão/SC; P6 - NB$_{PAI}$: *Nitossolo Bruno* in Painel/SC; P7 - LV$_{CAS}$: *Latossolo Vermelho* in Cascavel/PR. [2] Hor: horizon. -: not measured.

Pure clay minerals are characterized by one kind of cell unit only, so they have a full series of *00l* reflections with similar enlargements, controlled mainly by the thickness of the crystal, according to the Scherrer equation (Środoń et al., 2006). This means that pure kaolinite should show an integral set of peaks, for example, 0.712 nm (n = 1), 0.356 (n = 2), and 0.237 nm (n = 3). This premise is not followed in the soils studied since the position of the peaks in the *002* plan (d$_{002}$) does not obey an integral range, as shown in table 3 for the total clay samples.

In addition, *001* and *002* reflections are broad and asymmetrical, as exemplified in figure 3, where the best simulation of the shape of these two peaks is shown. In this case, the kaolinite peak positions were simulated for each plan at the points of greatest acuteness (summit) in 0.718 and 0.356 nm, respectively, and one more peak was introduced on both sides of them, theoretically simulating the existence of another mineral. This device allows us to clearly observe the strong asymmetry of the two "kaolinite" peaks, often indicative of interstratified kaolinite-smectite minerals, as found by many authors (Azevedo and Vidal-Torrado, 2009; Melo et al., 2009; Fiore et al., 2010).

Another doubt regarding the single presence of kaolinite in the samples of expansive soils is the excessively high values of WHH$_{001}$, which ranged from 0.66 to 0.97° 2θ. Thus, as the WHH$_{001}$ is calculated by the average peak position in the *001* plan, the bigger the WHH$_{001}$ (artificialized by the strong asymmetry), the lower the value of the MCD$_{001}$, according to Scherrer's equation, resulting in a small number of layers (ANL) in the crystals (Table 3). Considering the data in the literature, the values obtained for MCD$_{001}$ and ANL are smaller, and the WHH$_{001}$ is much higher than the kaolinite referred to in most international soils and in several soils in Brazilian environments (Melo et al., 2002; Corrêa et al., 2008). These authors indicate MCD$_{001}$ intervals with values between 20.3 and 27 nm, ANL between 28.3 and 37.5, and WHH$_{001}$ between 0.29 and 0.39 for kaolinite of soils derived from sedimentary rocks. The higher WHH$_{001}$ and the considerable asymmetry observed in expansive capacity are related to the 2:1 clay minerals and the presence of quasicrystals in these soils that can undergo dehydration in the interparticle porosity (porosity between

quasicrystals) and intraparticle porosity (pores between sub-units of quasicrystals and the interlayer space), reducing their size in the system. This effect promotes cohesion between adjacent particles, domains, and quasicrystals, leading to increased stacking of the particles. Upon rewetting or hydration of the particles, the domains and quasicrystals that were originally separated remained together, forming thicker microstructural units with fewer total pores. That way, the hydration and dehydration of these structures can be related to the higher WHH_{001} in the 2:1 expansive clay minerals and interstratified minerals present in the soils (Coulombe et al., 1996).

Therefore, the contrasting characteristics of the (supposed) kaolinites studied for MCD_{001}, ANL, and WHH_{001} in relation to other soil kaolinites, together with strong asymmetry of the two main peaks of "kaolinite" for lower angles, all suggest that the reflections at the position around 0.72 and 0.36 nm are not due only to the presence of kaolinites. Instead, they may be indicative of the contribution of interstratified clay minerals, possibly of the kaolinite-smectite (K-S) kind, since interstratified kaolinite-vermiculite is of rare occurrence, according to Wada and Kakuto (1983).

Furthermore, in relation to the crystallographic parameters, the asymmetric index (AI) for the A and B horizons of total, fine, and coarse clay fraction samples were calculated (Table 3), based on the considerations and results obtained by Melo and Wypych (2009). These authors suggest that this parameter can be a complementary means for identifying 2:1 interstratification layers in the kaolinite crystals.

In the samples of expansive soils, the AI values for the total clay fraction ranged from 0.14 to 0.38 nm, for fine clay from 0.10 to 0.24 nm, and for coarse clay from 0.16 to 0.42 nm, indicating high asymmetry of the peaks. Much lower values were obtained for non-expansive soil samples from Cascavel, where asymmetry indexes range from 0.08 to 0.13 nm for total clay, from 0.12 to 0.16 nm for fine clay, and from 0.21 to 0.24 nm for coarse clay (Table 3). Based on the hypothesis that higher values of the asymmetry index are related to a higher amount of interstratified K-S, it can be suggested that the amounts of K-S are much larger in brown expansive soil than in the non-expansive *Latossolo Vermelho* (Oxisol) from the state of Paraná.

Estimation of interstratified clay minerals

The amount of interstratified K-S estimated was high in most samples, except for the non-expansive Rhodic Hapludox from Cascavel. For the samples of expansive soil, K-S represented 41 to 51 % of the clay minerals traditionally interpreted as being only low crystallinity kaolinites with high structural disorder. Instead, in the Rhodic Hapludox from Cascavel, the estimated amount of interstratified minerals was much lower, 20 % in the A horizon and 30 % in the B horizon (Table 4). The higher amounts of K-S in the NB_{CUR} (A and B horizons), NB_{PS} (B horizon), and NB_{PAI} (A and B horizons) soils suggest that they have greater shrinkage capacity. This corroborates the results obtained by Silva (2015), where these same soils are classified as very expansive and expansive, according to cluster analysis (Table 5).

Therefore, it is plausible to hypothesize that the shrinkage characteristics of Oxisols from southern Brazil are due to two main factors: the contribution of significant amounts of 2:1 layer phyllosilicates (HIS), along with the interstratified K-S that are minerals with contraction-expansion properties, although limited by the presence of hydroxy-Al interlayer polymers; and the contribution of quasicrystals and domains in soils with 2:1 expansible minerals. These terms refer to the regions of preferential alignment of crystals or particles. In other words, domain is defined as microaggregation of crystallites in a more or less oriented arrangement, and the stacking of these crystallites creates pores inside the aggregate in which water may fill or penetrate (Coulombe et al., 1996). Thus, the water entering in the quasicrystalline structure is closely related to the contraction-expansion mechanisms mentioned and may be responsible for part of these effects.

Table 4. Values of the minerals that compose the samples, estimated by NEWMOD® software for the A and B horizons of the profiles studied, in the total clay fraction

Profile[1]	Horizon	2:1 HI Mineral	Kaolinite	K-S	Gibbsite[2]
			%		
P1 - LB_VAC	A	26	43	31	-
	B	23	39	38	-
P2 - LV_CN	A	22	41	37	-
	B	20	40	40	-
P3 - NB_CUR	A	20	40	40	-
	B	16	41	43	-
P4 - NB_PS	A	30	34	36	-
	B	17	41	42	-
P5 - LB_VAR	A	22	38	40	-
	B	24	38	38	-
P6 - NB_PAI	A	24	38	38	-
	B	21	39	40	-
P7 - LV_CAS	A	24	49	12	15
	B	30	31	13	26

[1] P1 - LB_VAC: *Latossolo Bruno* in Vacaria/RS; P2 - LV_CN: *Latossolo Vermelho* in Campos Novos/SC; P3 - NB_CUR: *Nitossolo Bruno* in Cutitibanos/SC; P4 - NB_PS: *Nitossolo Bruno* in Ponte Serrada/SC; P5 - LB_VAR: *Latossolo Bruno* in Vargeão/SC; P6 - NB_PAI: *Nitossolo Bruno* in Painel/SC; P7 - LV_CAS: *Latossolo Vermelho* in Cascavel/PR.
[2] Gibbsite: calculated values based on the percentage obtained by High Score Plus. -: not measured.

Table 5. Summary of results for the shrinkage indexes of the soils by the Syringe Method - COLEmod (Coefficient of linear extensibility), Metallic Mercury Method - DC (Degree of contraction of soil), and the Ring Filling Sand Method - RI (Shrinkage Index).

Profile[1]	Horizon	COLEmod[2]	DC[3]	RI
			%	
P1 - LB_VAC	A	0.14	0.13	0.06
	B	0.15	0.19	0.08
P2 - LV_CN	A	0.14	0.22	0.06
	B	0.17	0.25	0.07
P3 - NB_CUR	A	0.22	0.27	0.10
	B	0.20	0.28	0.08
P4 - NB_PS	A	0.20	0.27	0.08
	B	0.22	0.22	0.12
P5 - LB_VAR	A	0.14	0.13	0.06
	B	0.15	0.19	0.08
P6 - NB_PAI	A	0.18	0.28	0.12
	B	0.19	0.31	0.10
P7 - LV_CAS	A	0.16	0.14	0.02
	B	0.14	0.01	0.03

[1] P1 - LB_VAC: *Latossolo Bruno* in Vacaria/RS; P2 - LV_CN: *Latossolo Vermelho* in Campos Novos/SC; P3 - NB_CUR: *Nitossolo Bruno* in Cutitibanos/SC; P4 - NB_PS: *Nitossolo Bruno* in Ponte Serrada/SC; P5 - LB_VAR: *Latossolo Bruno* in Vargeão/SC; P6 - NB_PAI: *Nitossolo Bruno* in Painel/SC; P7 - LV_CAS: *Latossolo Vermelho* in Cascavel/PR.
[2] COLEmod (Schaefer and Singer, 1976). [3] Metallic Mercury Method - DC (Haluschak, 2006).

Quantification of fine clay and coarse clay fractions

For most of the samples studied, there was dominance of the fine clay over the coarse clay fraction (Table 6), with the exception of the A horizon of profile 1 - LB_VAC, where the coarse clay was slightly higher than the fine. These results are consistent with the considerations of Quirk and Aylmore (1971) and Tessier (1984), who argue that although a current conception is that the variation in volume of soils with a high content of expansive 2:1 phyllosilicates is due to variation in the volume of these minerals themselves, it is more plausible that the origin of these variations in volume is related to the dynamics of the water in the pores with diameters in the order of 1 to 2 µm that are created between quasicrystals and domains (the coarse clay fraction has a diameter between 0.2 and 2.0 micrometers).

Table 6. Quantification of the fine and coarse clay sub-fractions for the A and B horizons of the profiles studied.

Profile[1]	Horizon	Fine clay	Coarse clay
		%	
P1 - LB$_{VAC}$	A	49	51
	B	74	26
P2 - LV$_{CN}$	A	59	41
	B	56	44
P3 - NB$_{CUR}$	A	68	32
	B	73	27
P4 - NB$_{PS}$	A	71	29
	B	71	29
P5 - LB$_{VAR}$	A	68	32
	B	90	10
P6 - NB$_{PAI}$	A	62	38
	B	80	20
P7 - LV$_{CAS}$	A	82	18
	B	76	24

[1] P1 - LB$_{VAC}$: *Latossolo Bruno* in Vacaria/RS; P2 - LV$_{CN}$: *Latossolo Vermelho* in Campos Novos/SC; P3 - NB$_{CUR}$: *Nitossolo Bruno* in Cutitibanos/SC; P4 - NB$_{PS}$: *Nitossolo Bruno* in Ponte Serrada/SC; P5 - LB$_{VAR}$: *Latossolo Bruno* in Vargeão/SC; P6 - NB$_{PAI}$: *Nitossolo Bruno* in Painel/SC; P7 - LV$_{CAS}$: *Latossolo Vermelho* in Cascavel/PR.

The intense cracking observed in Oxisols in higher altitude regions in southern Brazil may therefore also be related to the crystallite arrangement of small dimension kaolinites that give rise to a flexible microstructure responsible for contraction and expansion of the soil with variation in moisture (Kämpf et al., 2012), although this does not exclude the influence of 2:1 minerals and interstratified K-S, as previously demonstrated. Nevertheless, we cannot exclude the properties related to landscape, relief, and topography, which are dominated by geomorphology.

Correlations between the physical and mineralogical soil properties

Analyzing a study on physical properties related to the expansive capacity of Oxisols from southern Brazil (Silva et al., 2017) and correlating this with the mineralogical properties, the methods that best simulated shrinkage capacity were the Degree of Contraction (DC) and the Shrinkage Index (RI), followed by the modified Coefficient of Linear Extensibility (COLE$_{mod}$).

Among the three indexes for evaluation of soil shrinkage, the one with the best correlation with the parameters of WHH$_{001}$, MCD$_{001}$, and ANL was DC 105 °C, followed by IR. The index with the lowest correlation was the COLEmod, which was statistically insignificant (Table 7). The higher WHH001 was also related to the higher DC and RI. However, for the MCD$_{001}$ and ANL, the behavior was inversely proportional. In this respect, in evaluating the relationship between physical properties and shrinkage capacity, Silva et al. (2017), using the same soils as in this study, attributed the lower efficiency of the COLEmod in estimating the shrinkage ability to the fact that it uses disturbed soil samples and is artificially prepared.

The results are consistent and partially confirm the central hypothesis of the study regarding the contribution of interstratified minerals to the shrinkage characteristics. The high values of WHH$_{001}$, as mentioned previously, are related not only to the presence of the kaolinite mineral, but also to the participation of non-regular interstratified K-S minerals. The main peaks of these minerals occurred close to the kaolinite *001* peaks and overlapped them, forming a single peak that is broad and asymmetrical for lower 2θ angles, which is generally interpreted as small size and highly disordered kaolinite. The more significant values of the asymmetry index (AI) for expansive soils compared to non-expansive soil are also indicative of the participation of interstratified K-S in most samples. This leads to the

Table 7. Pearson correlations between the expansive index of modified COLE (COLEmod), Degree of Contraction (DC), and Shrinkage Index (RI) with crystallographic parameters of "kaolinite" (d_{001}, WHH_{001}, MCD_{001}, ANL, and AI) and with the quantities of each clay mineral, semi quantified (g kg^{-1}) based on the amount of clay in each soil

	DC	RI	d_{001}	WHH_{001}	MCD_{001}	ANL	AI	2:1 HI	K	K-S	K-S + 2:1 HI
COLEmod	0.656*	0.647*	0.584*	0.407	-0.49	-0.498	0.492	-0.324	0.0592	0.362	0.26
	(0.0109)	(0.0124)	(0.0283)	(0.149)	(0.0755)	(0.0701)	(0.074)	(0.258)	(0.841)	(0.203)	(0.369)
DC	-	0.741*	0.601*	0.614*	0.685**	0.684**	0.386	-0.608*	-0.062	0.594*	0.388
	-	(0.0024)	(0.0231)	(0.0195)	(0.0068)	(0.007)	(0.173)	(0.0209)	(0.833)	(0.025)	(0.17)
RI	-	-	0.657*	0.559*	-0.587*	-0.598*	0.553*	-0.436	-0.111	0.685**	0.583*
	-	-	(0.0107)	(0.0377)	(0.0273)	(0.0239)	(0.0405)	(0.119)	(0.706)	(0.0068)	(0.0287)

* and **: significant at 5 and 1 % probability, respectively. Values in parentheses represent the probability index.

conclusion that there should be a relation between the AI and shrinkage index determined for each of the methodologies. However, the AI correlated positively and significantly only with the RI (Table 7), which partially confirms this presupposition.

The three shrinkage indexes were also compared to the crystallographic parameters of kaolinite in the fine clay (data not shown), and the correlations were more expressive than in the total clay, possibly due to the finer fraction. The peak area at 0.72 nm was significantly superior than in the total clay, and the asymmetry of the peaks in this position were better defined, which allowed the crystallographic parameters of the supposed kaolinite to be evaluated in detail.

When the shrinkage indexes were compared with the amounts of clay minerals in each soil horizon, the amounts of 2:1 HI phyllosilicates were negatively correlated only with the DC (Table 7). This is contradictory, since it could be indicating that shrinkage of the soil decreases with an increase in the minerals that swell. However, when these same indexes were compared with the amounts of interstratified K-S minerals, a positive correlation was observed with the DC and RI, indicating a significant correlation between these minerals and the indexes.

Although these correlations were positive, with significance levels lower than 5 % for DC and lower than 1 % for RI, they do not exclude other factors that may contribute to the shrinkage properties of the soils studied. As Quirk and Aylmore (1971) and Tessier (1984) suggest, the shrinkage characteristics may also be related to the water dynamics in very small pores due to the disordered arrangement of the kaolinite crystallites or of the interstratified K-S. This is plausible, considering the large amount of energy required to eliminate the water present in the interlayer of expansive minerals, which is lower if the water lost during the normal soil moistening and drying cycles in a natural environment is considered. This requires more investigation.

CONCLUSIONS

In qualitative analysis, the samples from the A and B horizons of the shrinkage soils studied showed similar mineralogical assembly in the clay fraction, with a predominance of kaolinite, interstratified kaolinite-smectite (K-S), and hydroxy-Al interlayered smectite (2:1 HIS). Gibbsite, goethite, and hematite occurred as minor components.

Broad and asymmetric peaks in the positions around 0.72 and 0.36 nm showed very high WHH_{001}, very low MCD_{001}, and an extremely small Average Number of Layers, incompatible with the crystallographic parameters referring to kaolinite that are found in different global environments.

The modeling of the X-ray diffractograms using the NEWMOD® software showed that most of the peaks normally assigned to kaolinite are due to the presence of kaolinite in association with interstratified kaolinite-smectite, whose quantities were more significant in the shrinkage soils.

The mineralogy of the clay fraction exhibited a relationship with the shrinkage properties of the soils, especially with the interstratified amount of K-S and the presence of the quasicrystals and domains; however, this does not exclude a possible contribution from landscape geomorphology and other factors.

ACKNOWLEDGMENTS

REFERENCES

Almeida JA, Maçaneiro KC, Klamt E. Mineralogia da fração argila de solos vermelhos com horizontes superficiais brunados do Planalto de Lages (SC). Rev Bras Cienc Solo. 2000;24:815-28. https://doi.org/10.1590/S0100-06832000000400014

Azevedo AC, Vidal-Torrado PV. Esmectita, vermiculita, minerais com hidróxi entrecamadas e clorita. In: Melo VF, Alleoni LRF, editores. Química e Mineralogia do Solo. Viçosa, MG: Sociedade Brasileira de Ciência do Solo; 2009. Pt 1. p.381-426.

Barnhisel RI, Bertsch PM. Chlorites and hydroxy-interlayered vermiculite and smectite. In: Dixon JB, Weed SB, editors. Minerals in soil environments. 2nd ed. Madison: Soil Science Society of America; 1989. p.729-88.

Benedetti UG, Vale Júnior JF, Schaefer CEGR, Melo VF, Uchôa SCP. Gênese, química e mineralogia de solos derivados de sedimentos pliopleistocênicos e de rochas vulcânicas básicas em Roraima, Norte Amazônico. Rev Bras Cienc Solo. 2011;35:299-312. https://doi.org/10.1590/S0100-06832011000200002

Brown G, Brindley GW. X-ray diffraction procedures for clay mineral identification. In: Brindley GW, Brown G, editors. Crystal structures of clay minerals and their X-ray identification. London: Mineralogical Society; 1980. p.305-60.

Brown G, Newman ACD, Rayner JH, Weir AH. The structures and chemistry of soil clay minerals. In: Greeland DJ, Hayes MHB, editors. The chemistry of soil constituents. Chichester: John Wiley & Sons; 1978. p.29-178.

Churchmann GJ, Slade PG, Self PG, Janik LJ. Nature of interstratified kaolinite-smectites in some Australian soils. Austr J Soil Res. 1994;32:805-22. https://doi.org/10.1071/SR9940805

Coulombe CE, Dixon JB, Wilding LP. Mineralogy and chemistry of vertisols. In: Ahmad N, Mermut A. editors. Vertisols and technologies for their management. Amsterdam: Elsevier Science;1996. p.115-200.

Corrêa MM, Ker JC, Barrón V, Torrent J, Fontes MPF, Curi N. Propriedades cristalográficas de caulinitas de solos do ambiente Tabuleiros Costeiros, Amazônia e Recôncavo Baiano. Rev Bras Cienc Solo. 2008;32:1857-72. https://doi.org/10.1590/S0100-06832008000500007

Dudek T, Środoń J. Thickness distribution of illite crystal in shales. II: Origin of the distribution and the mechanism of smectite illitization in shales. Clays Clay Miner. 2006;51:529-42. https://doi.org/10.1346/CCMN.2003.0510507

Fiore S, Cuadros J, Huertas FJ. Interstratified clay minerals: origin, characterization and geochemical significance. Bari: Aipea Educational Series; 2010.

Giarola NFB, Lima HV, Romero RE, Brinatti AM, Silva AP. Mineralogia e cristalografia da fração argila de horizontes coesos de solos nos tabuleiros costeiros. Rev Bras Cienc Solo. 2009;33:33-40. https://doi.org/10.1590/S0100-06832009000100004

Haluschak P. Laboratory methods of soil analysis. Canada-Manitoba soil survey; 2006. Available at: http://www.manitoba.ca/agriculture/land/soil-survey/pubs/laboratory_methods_of_soil_analysis.pdf.

Herbillon AJ, Frankart R, Vielvoye L. An occurrence of interstratified kaolinite-smectite minerals in a red-black soil toposequence. Clay Miner. 1981;16:195-201.

Jackson ML. Soil chemical analysis: advanced course. Madison: Parallel Press; 1965.

Kämpf N, Marques JJ, Curi N. Mineralogia dos solos brasileiros. In: Ker JC, Curi N, Schaefer CEGR, Vidal-Torrado P, editores. Pedologia - Fundamentos. Viçosa, MG: Sociedade Brasileira de Ciência do Solo; 2012. p.81-146.

Klug HP, Alexander LE. X-ray diffraction procedures for polycrystalline and amorphous materials. New York: John Wiley & Sons; 1954.

Lima Neto JA, Ribeiro MR, Corrêa MM, Souza-Júnior VS, Filho JCA, Lima JFWF. Atributos químicos, mineralógicos e micromorfológicos de horizontes coesos de Latossolos e Argissolos dos tabuleiros costeiros do estado de Alagoas. Rev Bras Cienc Solo. 2010;34:473-86. https://doi.org/10.1590/S0100-06832010000200021

Mehra OP, Jackson ML. Iron oxide removal from soils and clays by a dithionite-citrate system buffered with sodium bicarbonate. In: Swineford A, editor. Clays and Clay Minerals. London: Pergamon Press, 1960. p.317-27.

Melo VF, Mattos JMSM, Lima VC. Métodos de concentração de minerais 2:1 secundários na fração argila visando sua identificação por difratometria de raios X. Rev Bras Cienc Solo. 2009;33:527-39. https://doi.org/10.1590/S0100-06832009000300006

Melo VF, Wypych F. Caulinita e Haloisita. In: Melo VF, Alleoni LRF, editores. Química e Mineralogia do Solo. Viçosa, MG: Sociedade Brasileira de Ciência do Solo; 2009. Pt 1. p.427-504.

Melo VF, Schaefer CEGR, Singh B, Novais RF, Fontes MPF. Propriedades químicas e cristalográficas da caulinita e dos óxidos de ferro em sedimentos do Grupo Barreiras no município de Aracruz, estado do Espírito Santo. Rev Bras Cienc Solo. 2002;26:53-64. https://doi.org/10.1590/S0100-06832002000100006

Melo VF, Singh B, Schaefer CEGR, Novais RF, Fontes MPF. Chemical and mineralogical properties of kaolinite-rich Brazilian soils. Soil Sci Soc Am J. 2001;65:1324-33. https://doi.org/10.2136/sssaj2001.6541324x

Palmieri F. A study of a climosequence of soils derived from volcanic rock parent material in Santa Catarina and Rio Grande do Sul States, Brazil [thesis]. West Lafayette: Purdue University; 1986.

Quirk JP, Aylmore LAG. Domain and quasi-crystalline regions in clay systems. Soil Sci Soc Am J. 1971;35:652-4. https://doi.org/10.2136/sssaj1971.03615995003500040046x

Reynolds Jr RC. NEWMOD, a computer program for the calculation of one-dimensional diffraction patterns of mixed-layered clays. Hannover: Brook Rd; 1985.

Ryan PC, Huertas FJ, Hobbs FWC, Pincus LN. Kaolinite and halloysite derived from sequential transformation of pedogenic smectite and kaolinite-smectite in a 120 ka tropical soil chronosequence. Clays Clays Miner. 2016;64:639-67. https://doi.org/10.1346/CCMN.2016.064030

Santos HG, Jacomine PKT, Anjos LHC, Oliveira VA, Oliveira JB, Coelho MR, Lumbreras JF, Cunha TJF. Sistema brasileiro de classificação de solos. 3a ed. Rio de Janeiro: Embrapa Solos; 2013.

Schaefer WM, Singer MJ. A new method of measuring shrink-swell potential using soil pastes. Soil Sci Soc Am J. 1976;40:805-6. https://doi.org/10.2136/sssaj1976.03615995004000050050x

Silva L. Caráter retrátil de Nitossolos e Latossolos do Sul do Brasil [dissertação]. Lages: Universidade do Estado de Santa Catarina; 2015.

Silva L, Sequinatto L, Almeida JA, Bortolini D. Methods for quantifying shrinkage in Latossolos (Ferralsols) and Nitossolos (Nitisols) in Southern Brazil. Rev Bras Cienc Solo. 2017;41:1-12. http://doi.org/10.1590/18069657rbcs20160364

Środoń J, Kotarba M, Biroň A, Such P, Clauer N, Wójtowicz A. Diagenetic history of the Podhale-Orava Basin and the underlying Tatra sedimentary structural units (Western Carpathians): evidence from XRD and K-Ar of illite-smectite. Clay Minerals. 2006;41:751-74. https://doi.org/10.1180/0009855064130217

Teske R, Almeida JA, Hoffer A, Lunardi Neto A. Caracterização mineralógica dos solos derivados de rochas efusivas no Planalto Sul de Santa Catarina, Brasil. Rev Cienc Agrovet. 2013;12:187-98.

Tessier D. Estude experimentále de l'organisation des matériaux argilcux. Hydratation, gonflement et structuration au cours de la dessiccation et de la réhumectation [Ph. D thesis]. Paris, France: Universidade de Paris; 1984.

Wada K, Kakuto Y. Intergradient vermiculite-kaolin mineral in a Korean Ultisol. Clays Clay Miner. 1983;31:183-90. https://doi.org/10.1346/CCMN.1983.0310303

Whittig LD, Allardice WR. X-ray diffraction techniques. In: Klute A, editor. Methods of soil analysis. Physical and mineralogical methods. 2nd ed. Madison: American Society of Agronomy; 1986. Pt 1. p.331-62.

Wilding LP, Tessier D. Genesis of Vertisols: shrink-swell phenomena. In: Wilding LP, Puentes R, editors. Vertisols: their distribution, properties, classification and management. College Station: Texas A&M University Printing Center; 1988. p.55-81.

Yerima BPK, Calhoun FG, Senkayi AL, Dixon JB. Occurrence of interstratified kaolinite-smectite in El Salvador Vertisols. Soil Sci Soc Am J. 1984;49:462-6. https://doi.org/10.2136/sssaj1985.03615995004900020038x

Yongue-Fouateu R, Ndimukong F, Njoya A, Kunyukubundo F, Mbih PK. The Ndop plain clayey materials (Bamenda area – NW Cameroon): mineralogical, geochemical, physical characteristics and properties of their fired products. J Asian Ceramic Soc. 2016;4:299-308. https://doi.org/10.1016/j.jascer.2016.05.008